Cell-Penetrating Molecules

DOI: 10.1002/anie.200600312

Design, Synthesis, and Membrane-Translocation Studies of Inositol-Based Transporters**

*Kaustabh K. Maiti, Ock-Youm Jeon, Woo Sirl Lee, Dong-Chan Kim, Kyong-Tai Kim, Toshihide Takeuchi, Shiroh Futaki, and Sung-Kee Chung**

Cell membrane systems represent formidable physical barriers for the trafficking of unintended molecules. Only those molecules with an appropriate range of molecular size, polarity, and charge are allowed to pass through cell membranes. Many potential drug molecules have to overcome these barriers, and a variety of chemical and physical methods have been proposed as means of accomplishing this challenging task. A number of peptides have been reported to

[*] Dr. K. K. Maiti, O.-Y. Jeon, W. S. Lee, Prof. Dr. S.-K. Chung
Department of Chemistry
Pohang University of Science and Technology
Pohang 790-784 (Korea)
Fax: (+82) 54-279-3399
E-mail: skchung@postech.ac.kr

D.-C. Kim, Prof. Dr. K.-T. Kim
Department of Life Science
Pohang University of Science and Technology
Pohang 790-784 (Korea)

T. Takeuchi, Prof. Dr. S. Futaki
Department of Biofunctional Chemistry
Institute for Chemical Research
Kyoto University
Uji, Kyoto 611-0011 (Japan)
and
PRESTO
Japan Science and Technology Corporation (JST)
Kawaguchi, Saitama 332-0012 (Japan)

[**] We thank Dr. Hyun Soo Kim for technical assistance with cell cultures, MTT tests, and operation of the confocal laser scanning microscope at Postech. Financial support from Postech, Posco (Postech Biotech Center), BK-21, and MOST (National Frontier Research Program administered through KRICT/CBM), and Grants-in Aid for Scientific Research from the Ministry of Education, Culture, Sports, Science, and Technology of Japan is gratefully acknowledged.

Supporting information for this article is available on the WWW under http://www.angewandte.org or from the author.

translocate themselves across cell membranes. They are known as cell-penetrating peptides or protein transduction domains, and are capable of delivering exogenous molecules into cells. The first cell-membrane-penetrating property was observed with HIV-1 Tat protein (Tat-86) and then with the antennapedia (Antp) protein of *Drosophila* and others. Subsequent studies have demonstrated that the membrane-penetrating ability is clearly associated with relatively short peptide sequences in these proteins; for example, nine basic amino acid residues for the Tat protein (residues 49–57), 16 amino acids for the Antp protein (residues 43–58) that have a potentially amphipathic and basic helical structure, and 12 hydrophobic amino acids from Kaposi's sarcoma fibroblast growth factor membrane-translocating sequence (KFGF-MTS).[1–4] Despite the lack of a clear understanding of the membrane-translocation mechanisms, many research efforts have been extended toward their applications as delivery vectors in order to improve the pharmacology of poorly bioavailable drugs, such as, small molecules,[5] proteins,[6–10] nucleotides, and genes.[11–13] Reports have also appeared on the development of membrane-translocating transporter molecules that mimic natural and non-natural amino acids and their structural analogues, especially in the area of polycationic peptide mimetics.[14–23]

Although these peptides commonly share a high efficiency as molecular transporters, the structural motifs and physicochemical properties of these cell-penetrating peptides are quite diverse. It appears likely that different peptides may use variant mechanisms of translocation and that even the same peptide can use alternative pathways depending on conditions of administration and the nature of cargo, as was previously suggested.[10] Therefore, the modifications of the structures and physicochemical properties of even the known molecular transporters may yield novel transporters that exhibit different spectra in vivo and in vitro, as well as different translocation efficiencies. In addition, the in vivo efficacy, stability to various endogenous enzymes, processing cost, and long-term safety still remain practical concerns. With these considerations in mind, we have developed a novel class of molecular transporters as a potential delivery vector which consist of multiple units of the guanidine residue attached to the dimeric inositol molecule as a scaffold. Carbohydrate and inositol structures reveal the highest density of functionality among organic compounds per unit weight in the form of multiple hydroxy groups with diverse stereochemical variations. Also, they occur naturally and are largely devoid of any noticeable toxicity. Carbohydrates and inositols may provide an excellent platform to build a molecular diversity by appending desired structural residues around the scaffold. A number of research groups have previously attempted to design various peptidomimetics on the carbohydrate scaffolds.[24]

We prepared a number of synthetic transporter molecules by utilizing *myo*- and *scyllo*-inositol dimers as the scaffolds (Figure 1). Although *myo*-inositol is most abundant in nature and readily available, substitution at sites other than the C2 and C5 positions tends to generate a diastereomeric mixture, whereas *scyllo*-inositol, albeit less readily available, has a higher degree of symmetry with all equatorial hydroxy groups. We initially developed synthetic protocols with *myo*-inositol as the scaffold to give **1**, and then prepared the transporter **2** based on the *scyllo*-inositol scaffold (see Supporting Information for details of the syntheses of **1** and **2**).[25,26] Compounds **3a–c** were prepared as shown in Scheme 1. Compound **5**, prepared from 1-*O*-Bz-2,3:5,6-di-*O*-isopropylidene-*scyllo*-inositol[26] (see Supporting Information), was converted into **6** and **7**, and these two components were coupled using EDC, HOBT, and DMAP in DMF to give **8** in 65% yield. The compound **9**, obtained from **8** by removal of the isopropylidene protecting groups, was exhaustively acylated with *N*-Boc-protected 4-aminobutyric ($n=3$), 6-aminocaproic ($n=5$), and 8-aminocaprylic ($n=7$) acids, respectively, under EDC coupling conditions to give three dimeric products, **10a–c**, with varying chain lengths (see Scheme 1). Removal of the *N*-Boc protecting groups of **10a–c** exposed the terminal amino groups, which were guanidiny-

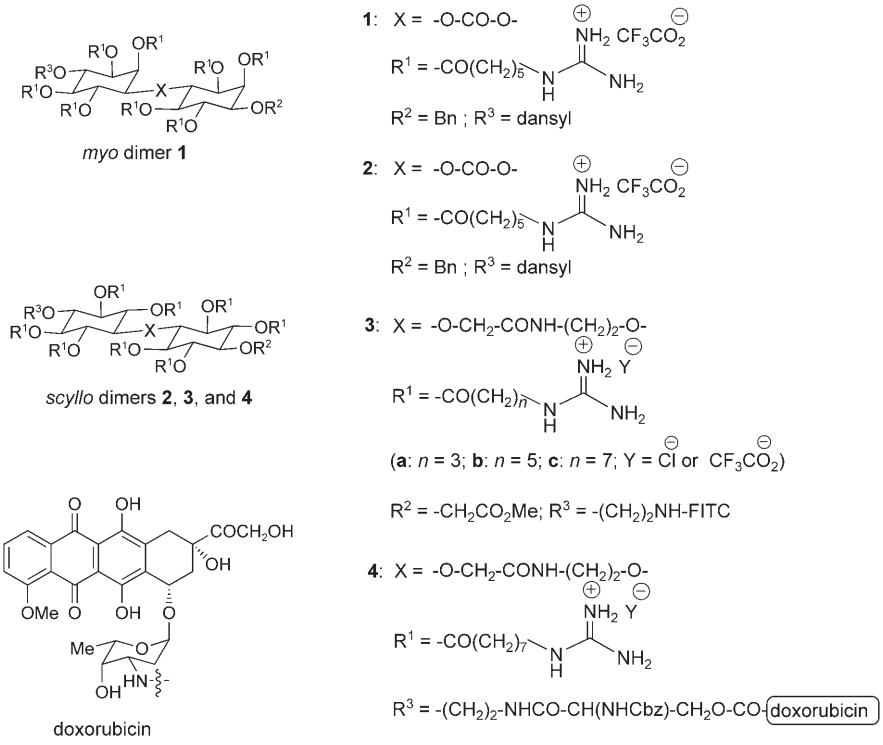

Figure 1. Structures of the synthetic molecular transporters **1–3** and a covalent conjugate of **3c** with doxorubicin, **4**. Cbz = carbobenzyloxy.

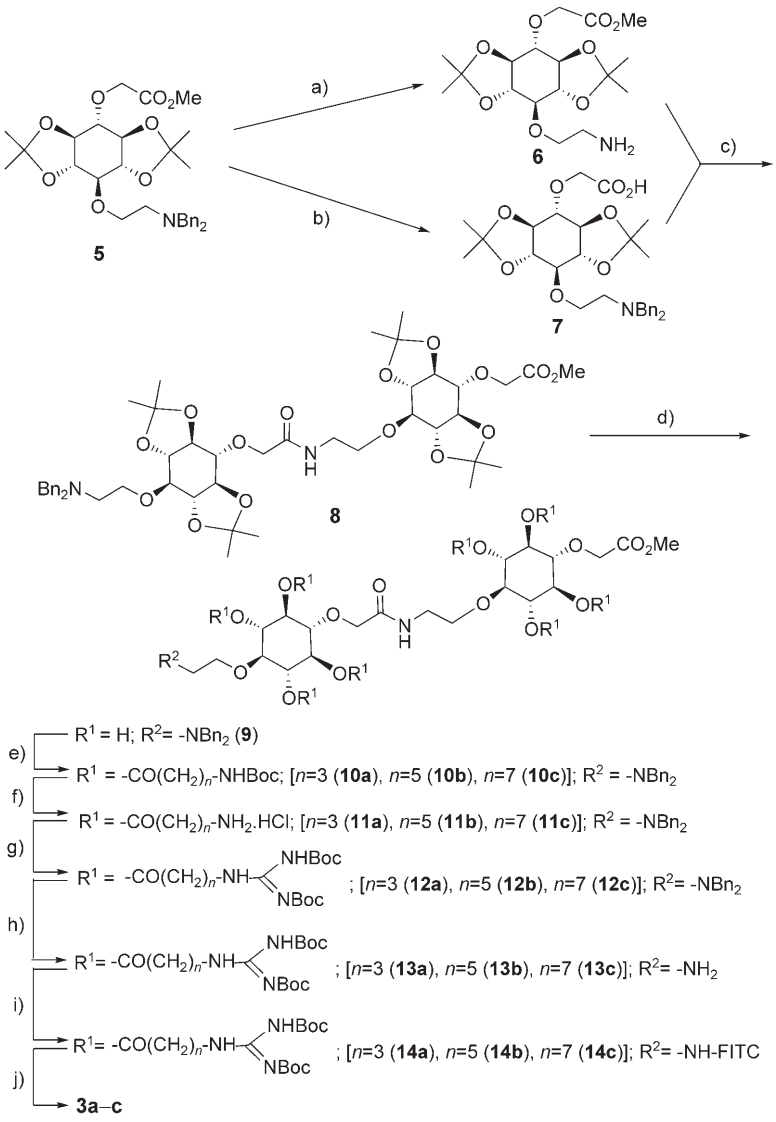

Scheme 1. Synthetic route to compounds **3a–c**. Reagents and conditions: a) 10% Pd/C, H_2 (1 atm), CH_2Cl_2/MeOH (1:9), quant.; b) NaOH, MeOH, then AcOH, 92%; c) **6**, **7**, EDC, HOBT, DMAP, DMF, 65%; d) *p*-TSA, CH_2Cl_2/MeOH (9:1), quant.; e) EDC, DMAP, *N*-Boc-protected acids: 4-aminobutyric acid ($n=3$), 6-aminocaproic acid ($n=5$), or 8-aminocaprylic acid ($n=7$), DMF, 65–80%; f) HCl(g), EtOAc, quant.; g) *N*,*N*′-di-Boc-*N*″-triflylguanidine, Et_3N, dioxane/H_2O (5:1), 55–76%; h) 10% Pd/C, H_2 (1 atm), MeOH/CH_2Cl_2 (9:1), 75–80%; i) FITC-I, Et_3N, THF, absolute EtOH, 52–65%; j) HCl(g), EtOAc, 76–80%; or TFA/CH_2Cl_2 (1:1), 86–94%. Bn = benzyl; EDC = 1-ethyl-3-(3-dimethylaminopropyl)-carbodiimide; HOBT = hydroxybenzotriazole; DMAP = 4-(dimethylamino)pyridine; DMF = *N*,*N*-dimethylformamide; *p*-TSA = *p*-toluenesulfonic acid; Boc = *tert*-butoxycarbonyl; FITC = fluorescein isothiocyanate; TFA = trifluoroacetic acid.

lated with a large excess of *N*,*N*′-di-Boc-*N*″-trifluoromethanesulfonylguanidine and triethylamine to give three target molecules, **12a–c**, with the Boc-protected guanidine moiety. After removal of the *N*-benzyl protecting group in the side chain of **12a–c**, the fluorescein tag was attached to the primary amino group of **13a–c** using fluorescein-5-isothiocyanate (FITC-I) and triethylamine to give **14a–c**. The Boc groups at the guanidine moieties in compounds **14** were removed with either trifluoroacetic acid or gaseous HCl to yield three molecular transporters, **3a–c**, as salts after purification by medium-pressure liquid chromatography (MPLC) on reverse-phase (C_8) silica gel.

For the preparation of a transporter–cargo conjugate, Cbz-protected L-serine was attached through an amide bond to the primary amine of compound **13c** under the EDC coupling conditions. The hydroxy group of the serine moiety was then coupled with the primary amino group of doxorubicin through a carbamate bond.[27] Finally the *N*-Boc protecting groups of the guanidine moieties were removed with gaseous HCl to yield the covalent conjugate **4** as its HCl salt (see Figure 1). All key synthetic intermediates as well as the final target compounds were satisfactorily characterized by NMR spectroscopy and MALDI-TOF mass spectrometry.

Preliminary evaluations of the synthetic transporters were carried out for their ability to translocate into the cytoplasm with three cell lines: COS-7, RAW264.7, and HeLa cells. After exposure of the cultured cells to the transporters for 3–5 minutes, cellular uptake of the four compounds **1**, **2**, **3b**, and **3c**, without fixing, was found to be more efficient than with the reference compounds, dansyl- and fluorescein-labeled nona-arginine (R9-Fl), on the basis of confocal laser scanning microscopy observations; compound **3a** appeared to be approximately as efficient as the reference standard. Thus, more detailed studies were carried out on HeLa cells with the more stable amide compounds **3a–c**. The internalization efficiencies of the transporters **3a–c** were compared with that of fluorescein-labeled octaarginine (R8-Fl), a representative cell-penetrating peptide. The HeLa cells were treated with the respective transporter (10 μM) at 37 °C for 1 h. Fluorescence-activated cell sorter (FACS) analysis of the transporters demonstrated that **3b** and **3c** were internalized 1.8 and 2.5 times as much as R8-Fl, whereas the amount of **3a** internalized was about half that of R8-Fl under the same conditions (Figure 2A). A more precise kinetics study of internalization was performed with the most efficient transporter **3c** in comparison with R8-Fl (Figure 2B). In contrast to the observation that the amount of R8-Fl internalized reached a plateau in 3 h, the internalization of **3c** kept increasing and did not reach a plateau in 6 h. The total cellular uptake of **3c** was almost three times higher than that of R8-Fl. However, no significant toxicity was evident for these cells.

The cellular (organellar) localizations of the transporter **3c** were examined next without fixing. First, HeLa cells were treated with **3c** (10 μM) at 37 °C for 1 h in the presence of tetramethylrhodamine-labeled transferrin (Rho-Tf) as a marker of clathrin endocytosis (25 $\mu g\,mL^{-1}$). Considerable fractions of both labels in punctate structures showed a

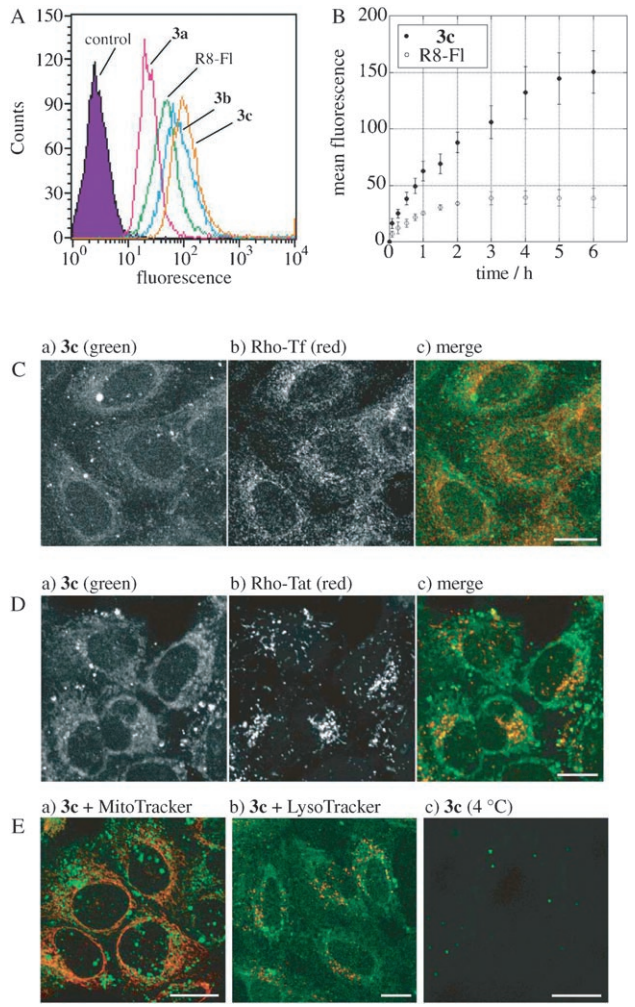

Figure 2. Cellular uptake studies of compound **3c** using HeLa cells. A) FACS analysis of the compounds **3a–c** taken up by HeLa cells. The cells were treated with compounds **3a–c** (10 μM each) in serum-containing minimum essential medium (MEM) at 37 °C for 1 h and were analyzed by FACS. B) Kinetics study of the amount of compound **3c** taken up by the cells in comparison with that of the fluorescein-labeled octaarginine (R8-Fl). The cells were incubated with compound **3c** or R8-Fl (10 μM each) at 37 °C for different time intervals and analyzed by FACS. C) Observation by confocal microscopy of the cells treated with **3c** (10 μM) in the presence of tetramethylrhodamine-labeled transferrin (Rho-Tf; 25 $\mu g\,mL^{-1}$) at 37 °C for 1 h. D) The cells were treated with **3c** and tetramethylrhodamine-labeled Tat peptide (Rho-Tat; 10 μM each) at 37 °C for 1 h. E): a) No significant colocalization of the signals of **3c** with MitoTracker (250 nM) is seen; b) the majority of **3c** did not reach the lysosome in 1 h (lysosomes were stained with 50 nM LysoTracker); c) no significant internalization was observed either for the cells treated with **3c** (10 μM) for 1 h at 4 °C. Scale bars: 20 μm. See text for details.

distinct localization pattern under the experimental conditions (Figure 2C). When the cells were similarly treated with **3c** at 4 °C, no significant internalization was observed (Figure 2E, part c). These results suggest that **3c** internalizes through an endocytic route that is different from the well-characterized clathrin-dependent pathway. Interestingly, **3c** may possibly internalize using pathways that are different even from those of the Tat peptide, another representative arginine-rich transporter. HeLa cells were treated with **3c** in the presence of tetramethylrhodamine-labeled Tat peptide (Rho-Tat; 10 μM each) at 37 °C for 3 h. Also, little colocalization of the signals of **3c** and Rho-Tat was observed. The majority of the signals from Rho-Tat were observed in the peripheries of the nucleus, whereas the wider spread signals of **3c** were observed in the cytosolic region. Moreover, as was previously observed, the Tat-positive structures were often considerably larger than those for **3c** (Figure 2D). We further examined whether **3c** was delivered into lysosomes or mitochondria by co-staining with specific dyes for lysosomes (LysoTracker) and mitochondria (MitoTracker), respectively (Figure 2E). No significant colocalization of the signals of **3c** with MitoTracker (250 nM) was observed (Figure 2E, part a), and the majority of **3c** did not reach the lysosome in 1 h (lysosomes were stained with 50 nM LysoTracker; see Figure 2E, part b). These results strongly suggest that **3c** may use different mechanisms of internalization and cellular localization from those transporters reported to date, even though it comprises a cluster of guanidinium moieties albeit on a dimeric inositol scaffold.

Next, we examined if compound **3c** also showed a unique in vivo biodistribution pattern. Thus, **3c** (HCl salt, 77 $mg\,kg^{-1}$) was dissolved in sterile distilled water and injected into 8-week-old mice (C57BL/6) intraperitoneally. After 20 minutes, the treated mice were perfused with 4% paraformaldehyde in phosphate buffer solution (PBS; pH 7.4), and the organs, including the heart, spleen, liver, kidneys, and lungs, cut into 15 μm sections, were incubated overnight in a solution of 0.5 M sucrose in PBS. After drying at 37 °C, the sections were washed with PBS and treated with 0.3% Triton X-100 at room temperature and analyzed by fluorescence microscopy. The Tat peptides were previously reported to show predominant tissue distribution in the liver, kidneys, lungs, heart muscle, and spleen.[23,28] In contrast to these observations, significantly lower extents of internalization of **3c** into the liver, kidney, and spleen were observed; **3c** was located only in the peripheries of these organs. However, much higher distributions of **3c** were seen in heart, lung, and brain tissues (Figure 3). Because of its potential implications on the possible selective delivery into the central nervous system, we specifically repeated the tissue distribution experiment of compound **3c** in the mouse brain at a dosage level of 57 $mg\,kg^{-1}$ for 20 minutes. The brain cortex region showed strong fluorescence, suggesting that the transporter indeed

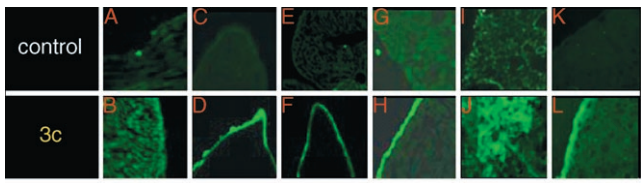

Figure 3. Distribution of **3c** (HCl salt) into mouse tissues. Fluorescence microscopy images (green fluorescence from FITC) of heart muscle (A, B), spleen (C, D), liver (E, F), kidney (G, H), and lung (I, J) tissue sections, and coronal brain sections (K, L) isolated from mice 20 minutes after intraperitoneal injection. Exposure time: 14000 ms (A, B); 500 ms (C, D); 300 ms (E, F); 500 ms (G, H); 1200 ms (I, J); 1000 ms (K, L); $\lambda_{em} = 488$ nm.

crossed the blood–brain barrier (BBB) rapidly and efficiently (see Supporting Information). Development of vectors to help cross the BBB is one of the major challenges in drug delivery, and these observations should be useful in the development of organ-selective delivery technologies.

Last, we investigated the in vitro and in vivo distribution of the transporter **3c**–doxorubicin conjugate **4**. Doxorubicin hydrochloride (adriamycin) is extensively used clinically for the treatment of a variety of neoplastic diseases, including leukaemia and breast, ovarian, and solid cancers, but not brain cancer, as it does not overcome the BBB.[29] Doxorubicin reveals strong UV/Vis absorption bands and is also highly fluorescent. Compound **4** was examined for its cell-penetrating ability with HeLa cells without fixing. The conjugate **4** at concentrations of 10 and 30 μM showed much-enhanced translocation into the cytoplasm when compared with doxorubicin itself (Figure 4 A). However, the cells

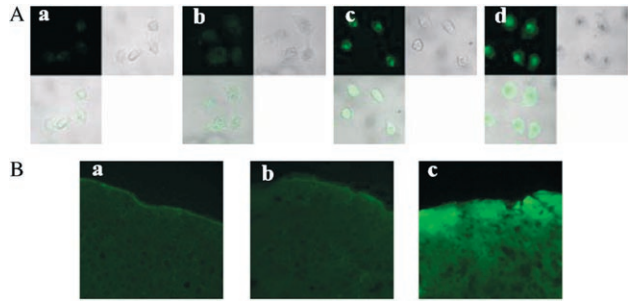

Figure 4. A) Fluorescence microscopy images of doxorubicin (green fluorescent emission) and doxorubicin–**3c** conjugate, **4**: a) doxorubicin (10 μM), b) doxorubicin–**3c** conjugate, **4** (HCl salt, 10 μM), c) doxorubicin (30 μM), and d) conjugate **4** (30 μM) in HeLa cells incubated for 15 minutes at 37 °C. B) Fluorescence microscopy images of mouse brain sections (cortex region): a) control (water), b) doxorubicin (21.3 mg kg^{-1}; M_r = 580 g mol^{-1}), and c) conjugate **4** (HCl salt, 115.8 mg kg^{-1}; M_r = 4452 g mol^{-1}). For part (B), sample treatment time: 20 minutes; exposure time: 9000 ms; λ_{em} = 488 nm.

treated with compound **4** showed changed morphologies, perhaps due to extensive cell death. Cell viability tests indeed indicated that the majority of the cells died at the dosage level of 10 μM of **4** after 24 h, whereas the same concentration of either doxorubicin or transporter **3c** alone caused no significant cell damage. This observation suggests that compound **4** was much more efficiently delivered into the cells compared to doxorubicin itself.

We further examined the uptake of free doxorubicin and the transporter–doxorubicin conjugate **4** into the brain. Thus, three mice (C57BL/6) were injected intraperitoneally with either sterile distilled water (0.5 mL, control), doxorubicin (21.3 mg kg^{-1}), or compound **4** (115.8 mg kg^{-1}) in the same volume of water. After 20 minutes, the mice were perfused with 4% paraformaldehyde in PBS (pH 7.4), and the brains were cut into 15 μm sections with a cryostat and incubated overnight in a solution of 0.5 M sucrose in PBS. After drying at 37 °C, the sections were washed with PBS and treated with 0.3% Triton X-100 at room temperature and analyzed by fluorescence microscopy. The fluorescence micrographs in Figure 4 B clearly show that a substantial amount of **4** is extensively distributed in the cortex region of the mouse brain (Figure 4 B, image c), whereas a very small amount of doxorubicin translocated into the brain cortex in the same timeframe (Figure 4 B, image b). These in vivo results suggest that the uptake of doxorubicin into the brain across the BBB is very inefficient, as expected, and that conjugation to the transporter **3c** significantly increases the uptake as well as the intercellular permeation of doxorubicin in the brain tissue.

In summary, the novel transporter structures based on dimeric inositol scaffolds reported here display unique spectra of distribution in vitro and in vivo. The lack of cell/organ specificities has generally been considered as one of the shortcomings of the Tat and oligoarginine-mediated delivery methods. However, the results shown here strongly suggest a possibility of designing highly sophisticated transporters by varying the structure of the backbone scaffold, charge densities, and perhaps other parameters. Thus, it is suggested that the structural diversity of sugars may be beneficial as scaffolds in the design of transporters in terms of not only aqueous solubility but also selective tissue and organellar distributions. Why the transporter **3c** shows these unique properties is not clear at this stage. Studies designed to provide additional information on these issues are in progress.

Received: January 24, 2006
Published online: March 23, 2006

Keywords: bioorganic chemistry · carbohydrates · drug delivery · fluorescence · membranes

[1] S. Futaki, *Adv. Drug Delivery Rev.* **2005**, *57*, 547.
[2] P. Ludberg, U. Langel, *J. Mol. Recognit.* **2003**, *16*, 227.
[3] A. Jolit, A. Prochiantz, *Nat. Cell Biol.* **2004**, *6*, 189.
[4] J. J. Schwartz, S. Zhang, *Curr. Opin. Mol. Ther.* **2000**, *2*, 162.
[5] J. B. Rothbard, S. Garlington, O. Lin, T. Kirschberg, E. Kreider, P. L. McGrane, P. A. Wender, P. A. Khavari, *Nat. Med.* **2000**, *11*, 1253.
[6] J. S. Wadia, S. F. Dowdy, *Curr. Protein Pept. Sci.* **2003**, *4*, 97.
[7] J. S. Wadia, R. V. Stan, S. F. Dowdy, *Nat. Med.* **2004**, *10*, 310.
[8] D. Jo, A. Nashabi, C. Doxsee, Q. Lin, D. Unutmaz, J. Chen, H. E. Ruley, *Nat. Biotechnol.* **2001**, *19*, 929.
[9] D. Jo, D. Liu, S. Yao, R. D. Collins, J. Hawiger, *Nat. Med.* **2005**, *11*, 892.
[10] I. Nakase, M. Niwa, T. Takeuchi, K. Sonomura, N. Kawabata, Y. Koike, M. Takehashi, S. Tanaka, K. Ueda, J. C. Simpson, A. T. Jones, Y. Sugiura, S. Futaki, *Mol. Ther.* **2004**, *10*, 1011.
[11] V. P. Tochilin, R. Rammohan, V. Weissig, T. S. Levchenko, *Proc. Natl. Acad. Sci. USA* **2001**, *98*, 8786.
[12] U. Krauss, M. Muller, M. Stahl, A. Beck-Sickinger, *Bioorg. Med. Chem. Lett.* **2004**, *14*, 51.
[13] K. Kogure, R. Moriguchi, K. Sasaki, M. Ueno, S. Futaki, H. Harashima, *J. Controlled Release* **2004**, *98*, 317.
[14] P. A. Wender, D. J. Mitchell, K. Pattabiraman, E. T. Pelkey, L. Steinman, J. B. Rothbard, *Proc. Natl. Acad. Sci. USA* **2000**, *97*, 13003.
[15] P. A. Wender, J. B. Rothbard, T. C. Jessop, E. L. Kreider, B. L. Wylie, *J. Am. Chem. Soc.* **2002**, *124*, 13382.
[16] J. B. Rothbard, E. Kreider, C. L. VanDeusen, L. Wright, B. L. Wylie, P. A. Wender, *J. Med. Chem.* **2002**, *45*, 3612.
[17] S. Futaki, T. Suzuki, W. Ohashi, T. Yagami, S. Tanaka, K. Ueda, Y. Sugiura, *J. Biol. Chem.* **2001**, *276*, 5836.

[18] S. Futaki, I. Nakase, T. Suzuki, Y. Zhang, Y. Sugiura, *Biochemistry* **2002**, *41*, 7925.
[19] N. Umezawa, M. A. Gelman, M. C. Haigis, R. T. Raines, S. H. Gellman, *J. Am. Chem. Soc.* **2002**, *124*, 368.
[20] N. Rueping, Y. Mahajan, M. Sauer, D. Seebach, *ChemBioChem* **2002**, *3*, 257.
[21] P. Zhou, M. Wang, L. Du, G. W. Fisher, A. Waggoner, D. H. Ly, *J. Am. Chem. Soc.* **2003**, *125*, 6878.
[22] N. W. Luedtke, P. Carmichael, Y. Tor, *J. Am. Chem. Soc.* **2003**, *125*, 12374.
[23] J. Fernandez-Carneado, M. Van Gool, V. Martos, S. Castel, P. Prados, J. de Mendoza, E. Giralt, *J. Am. Chem. Soc.* **2005**, *127*, 869.
[24] G. T. Le, G. Abbenante, B. Becker, M. Grathwohl, J. Halliday, G. Tometzki, J. Zuegg, W. Meutermans, *Drug Discovery Today* **2003**, *8*, 701.
[25] S. K. Chung, Y. H. Ryu, *Carbohydr. Res.* **1994**, *258*, 145.
[26] S. K. Chung, Y. U. Kwon, Y. T. Chang, K. H. Sohn, J. H. Shin, B. J. Hong, I. H. Chung, *Bioorg. Med. Chem.* **1999**, *7*, 2577.
[27] S. Sengupta, D. Eavarone, I. Capila, G. Zhao, N. Watson, T. Kiziltepe, R. Sasisekharan, *Nature* **2005**, *436*, 568.
[28] S. R. Schwarze, A. Ho, A. Vocero-Akbani, S. F. Dowdy, *Science* **1999**, *285*, 1569.
[29] C. R. Rousselle, M. Smirnova, P. Clair, J.-M. Lefauconnier, A. Chavanieu, B. Calas, J.-M. Scherrmann, J. Temsamani, *J. Pharmacol. Exp. Ther.* **2001**, *296*, 124.

